

breaking the continuity of the spinal cord and sanguination. After that, the fragments of oculomotoric muscles were taken. Part of the material was fixed in Baker's fluid for further ATP reaction according to the Wachstein and Meisel's method. Other sections of muscles were fixed in glutaraldehyde and OsO_4 and embedded in Epon 812. Ultrathin sections were contrasted by uranyl acetate and lead citrate according to the Reynold's method and were examined under electron microscope BS-500 (Tesla).

RESULTS

MICROSCOPIC OBSERVATIONS

Control group. Muscle fibre structure was typical of a cross-striated muscles. There were myosin microfilaments in the myofibrils seen as alongated fine striation, a very narrow striatum I (contraction phase) and electronically dense lines Z. Cisterns of smooth reticulum and distinct electronically dense lipid grains were visible among myofibrils, most often found separately or in pairs. Typical mitochondria with relatively developed crests were present too (Fig.1).

Experimental group I. Compared to the controls myofibrils in this group were less contracted. Thus striatum I was wider. The space among myofibrils was much wider with distinct disintegration of the smooth reticulum. Considerately constricted reticular cisterns and vesicles demonstrated the presence of lipid grains (Fig.2.).

Experimental group II. In this group of animals the space among myofibrils was very much shrunk so that the fibres nearly adhered to one another. Endoplasmic reticular membranes were hardly seen. Mitochondria presented normal structure but with better developed crests. They were tubular in shape and joined opposite walls of the structures. Mitochondrial matrix showed greater electronic density. Lipid grains were less numerous but glycogen grains were present in many places. The nuclear membrane was much folded in the form of finger-like projections into the cytoplasm and cytoplasmic indentations into the nuclear matrix. Heterochromatin formed smaller concentrations at the nuclear wall in comparison to the control animals.

Experimental group III. In this group many myofibrils had their shape changed. Their diameter was bigger in the middle of the sarcomere, they were distinctly narrower at the level of striatum Z and very narrow at striatum I (Fig.5). These fibres were fragmented and in atrophy in many places (Fig.6). Smooth reticular membranes were scarce, their "trace" fragments were observed in many sites. Pathologically changed mitochondria were also present. Some of them were very long, others irregularly bent (Fig.6). The longer seemed to have been formed of several smaller ones. Those much

deformed contained vacuoles surrounded by a double membrane. The mitochondria whose vacoules were extremely large, broke. Chromatin inside the nuclei was more rarified, with no chromatin at all at places. The concentration of heterochromatin at the folded nuclear surrounding membrane was much smaller than in groups I and II.

Experimental group IV. Pathological changes in this group reminded of group III, but were more advanced. The number of damaged mitochondria and myofibrils was greater than in group III. Especially mitochondria showed much advanced degeneration manifested as crest atrophy and the presence of large vacuoles.

ATP-ASE DETECTION

Control group. Distinct reaction in the form of a dark ring, manifestation of ATP-ase activity, was observed in the endomysium, around individual muscle fibres. ATP-ase activity was also detected in the connective tissue surrounding nerve fibres and in the vascular walls, especially in the endothelium (Fig.7,8).

Experimental animals. In the experimental groups I and II the reaction to ATP-ase was more intense in comparison to the controls (Fig.9). But in groups III and IV it was much weaker (Fig.10).

DISCUSSION

The onset of pathological changes due to diabetes is first manifested by vascular changes. They affect all vessels. In the large vessels they remind of atheromatomas, in the capillaries they result in a considerate proliferation of the basilar membrane. In the capillary walls, where there are no pericytes, microaneurysms formation occurs, e.g. within the retina. They may cause haemorrhages and necrotic foci (3). Damage to the capillary walls results in worse oxygenation and nourishment of the organs. The advancement of these changes depends mainly on the duration time of the disease.

In our experiment the changes in the ultrastructure of oculomotoric muscles were observed as early as 3 weeks after alloxan administration. They mainly concerned damage of the smooth reticulum which performs an important function in contraction, being the storage place of ions Ca^{++} . The striata in the sarcomeres were less visible, and striatum I got widened in comparison to the controls. It may be concluded the contractibility of myofibrils was weaker. Ivanov et al. (1979) report on the weakened function and signs of ciliary muscle fatigue in children with diabetes.

In the 6-week group neither interspaces between myofibrils nor smooth reticular membranes were visible in the muscle fibres. Concractile fibres were tightly packed. However, glycogen concentrations were visible in many places, which at increased blood glycogen concentration could have been released from the vascular walls or more weakly

metabolised in the muscle fibre. Bodies reminding of glycogen concentrations were found in the Schwann's cells of demyelinated nerve fibres supplying the external eye muscles in mice with diabetes were observed by Pachter (1986).

In two experimental groups (3-week and 6-week) the reaction to ATP-ase was more intense than in the controls. It may be concluded the energetic processes connected with sodium-potassium pump in the cellular membrane got activated. Mitochondria in the muscles from these animals showed no signs of damage. Mitochondrial crests were even better developed than in the controls and the matrix was electronically darker. This type of mitochondrial picture is characteristic of low energetic states when the cells demand great amounts of ATP-ase.

It is difficult to explain the existence of distinct folds of the nuclear membrane compared to the controls. They may result from its shrinkage due to changed ion flow, more intense exchange with the cytoplasm or other metabolic changes.

The damage to the oculomotoric muscles was pretty distinct after 3 months from alloxan administration. First of all, many myofibrils were degenerated. Broken continuity of fibres, their considerable narrowing or laceration were observed at the place of damage. There were normal fibres observed aside those damaged.

Mitochondria also showed distinct pathological changes such as irregular branched shape or very large size. Some of them were swollen as they contained vacuoles of various size. Those with extremely large vacuoles had no mitochondrial crests.

Cellular nuclei presented distinct manifestations of damage: rarefaction of chromatin, "empty spots" in the nuclear matrix and considerably lesser concentrations of heterochromatin at the nuclear capsule. This kind of nuclear picture is characteristic of the advanced phase of damage when the mechanism of sodium-potassium pump does not function properly and water gets into the nucleus.

Pathological changes after 6 months were like those after 3 months, however, the number of damaged structures was bigger. Nearly all mitochondria and the majority of myofibrils showed features of degeneration. Kaffer (6) and Föllman et al. (1) report on progressive dystrophy and vasculopathy of the external eye muscles in patients with recurrent oedema of the cornea and diabetes.

Advanced degeneration of the oculomotoric muscles observed in our experiment impairs the process of vision to a considerable degree. Zamlynska et al. (9) report on the impaired muscular balance, impaired eye movement and bilateral impairment of vision in patients with diabetes. Paralysis of nerve fibres supplying the oculomotoric muscles is one of the causes of their contractile fibre atrophy. Zrustova et al. (11) and Pachter (7) described degenerative changes in the motoric bodies and myeline cover. Nerve fibre paralysis develops under the influence of microangiopathic and arteriosclerotic factors (10).

CONCLUSIONS

1. In the course of diabetes the smooth reticulum is the first to undergo degeneration in the eye external muscle fibres.
2. Subsequently mitochondria, myofibrils and cellular nuclei undergo degeneration.

REFERENCES

1. Follmann P. et al.: Ultrastructural changes in the external recti muscles in diabetes mellitus. *Doc. Ophthalmol.* 83/1/55, 1993.
2. Fukuda M.: Clinical arrangement of classification of diabetic retinopathy. *Tohoku J. Exp. Med.*, 141, 331, 1983.
3. Hartwig W.: *Endokrynologia praktyczna*, PZWL, Warszawa 1989.
4. Henricsson M. et al.: Diabetic retinopathy before and after cataract surgery. *B. J. Ophthalmol.*, 80, 789, 1996.
5. Ivanov D. F. et al.: Sostoianie funkcii akkomodacii u detei pri nekotorych endokrynnykh rasstroistwach. *Oftalmol. Zh.* 34/8/467, 1979.
6. Kafer O.: Recurrent corneal edema without ocular hypertension, pigment degeneration, combined with deafness, progressive dystrophy of the outer eye-muscles in a patient with proportional dwarfism and diabetes mellitus. *Albrecht-Von- Graefes-Arch-Klin-Exp-Ophthalmol.*, 22,153,1977.
7. Pachter Br.: Structural alterations of the intramuscular nerves and junctional region and extraocular muscles of C57 Bl/Ks db/db diabetic mice. *Acta Neuropathol., Berl.* 72/2/164, 1986
8. Stevens V. J. et al.: Diabetic cataract formation: Potential role of glycosylation of lens crystallins. *Proc. Natl. Acad. Sci. USA*, 75, 2918, 1978.
9. Zamlynska A. et al.: Evaluation of binocular vision and eye balance in patients with diabetes. *Klin. Oczna*, 96/4-5/155, 1994.
10. Zorilla E., Kozak G.P.: Ophthalmoplegia in diabetes mellitus. *Ann. Intern. Med.*, 67/5/968, 1967.
11. Zrustova M. et al.: Diabetes changes of the extra-ocular-muscles in man. *Acta Diabetol.-Lat.*, 16/1/55, 1979.

STRESZCZENIE

Dojrzałym królikom podano jednorazowo alloksan w dawce 100 mg/kg m.c. Po 3 tyg., 6 tyg., 3 mies. i 6 mies. pobierano do badań mięśnie zewnętrzne gałki ocznej. Ultracienkie skrawki mięśni barwiono wg metody Reynoldsa i badano w mikroskopie elektronowym BS-500 firmy Tesla. Wykonano również odczyn na ATP-azę wg metody Wachsteina i Meisel.

Zmiany degeneracyjne obserwowano już po 3 tyg. i dotyczyły one siateczki śródplazmatycznej. Po 3 mies. stwierdzono uszkodzenie miofibrilli, mitochondriów i jądra komórkowego.

EXPLANATION TO FIGURES

Fig. 1. Longitudinal section of oculomotoric muscle in control rabbit. Visible are myofibrils, mitochondria, smooth reticulum, nucleus, electronically dense lipid grains. Mag. ca 14,000 x.

Fig. 2. Longitudinal section of oculomotoric muscle in rabbit from experimental group I. Visible are widened interspaces between myofibrils and disintegration of smooth endoplasmic reticulum. Mag. ca 14,000 x.

Fig. 3. Longitudinal section of oculomotoric muscle in rabbit from experimental group II. Visible are shrunk interspaces between myofibrils, glycogen concentrations and well developed mitochondrial crests. Mag. ca 14,000 x.

Fig. 4. Section of oculomotoric muscle in rabbit, experimental group II. Visible is much folded nuclear membrane. Glycogen grains are present between myofibrils. Mag. ca 14,000 x.

Fig. 5. Longitudinal section of oculomotoric muscle in rabbit, experimental group III. Visible are damaged myofibrils, fragments of endoplasmic reticulum and pathological long mitochondrion. Mag. ca 14,000 x.

Fig. 6. Section of oculomotoric muscle in rabbit, experimental group III. Visible are damaged myofibrils and pathological mitochondria. Mag. ca 10,000 x.

Fig. 7, 8. Longitudinal section (Fig. 7) and cross section (Fig. 8) of oculomotoric muscle of control rabbit. Visible is dark reaction to ATP-ase around fibres and nerves. Mag. ca 200 x.

Fig. 9. Longitudinal section of oculomotoric muscle in rabbit experimental group II. Very intense reaction around muscle fibres. Mag. ca 200 x.

Fig. 10. Longitudinal section of oculomotoric muscle in rabbit, experimental group IV. Visible is weak reaction to ATP-ase around muscle fibres. Mag. ca 200 x.

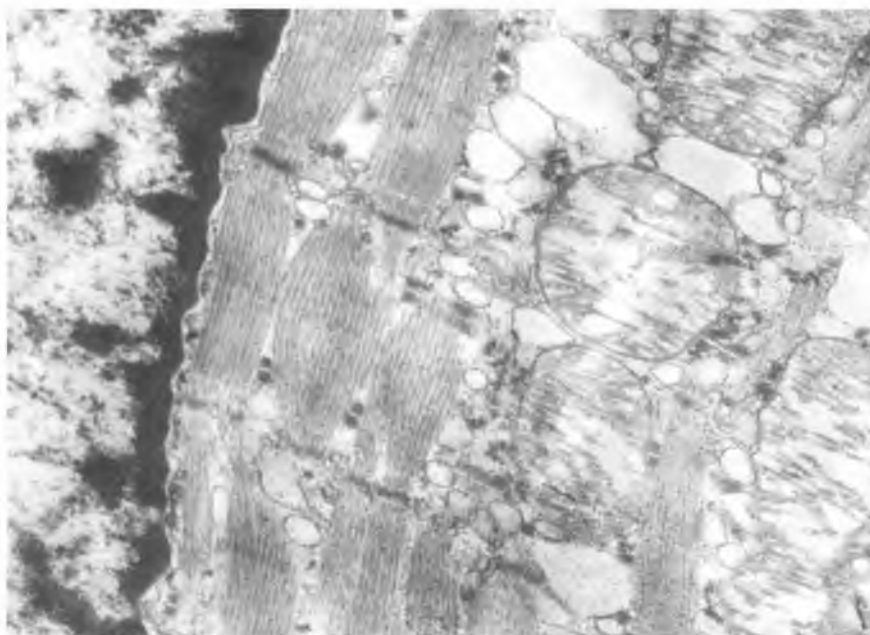


Fig. 1

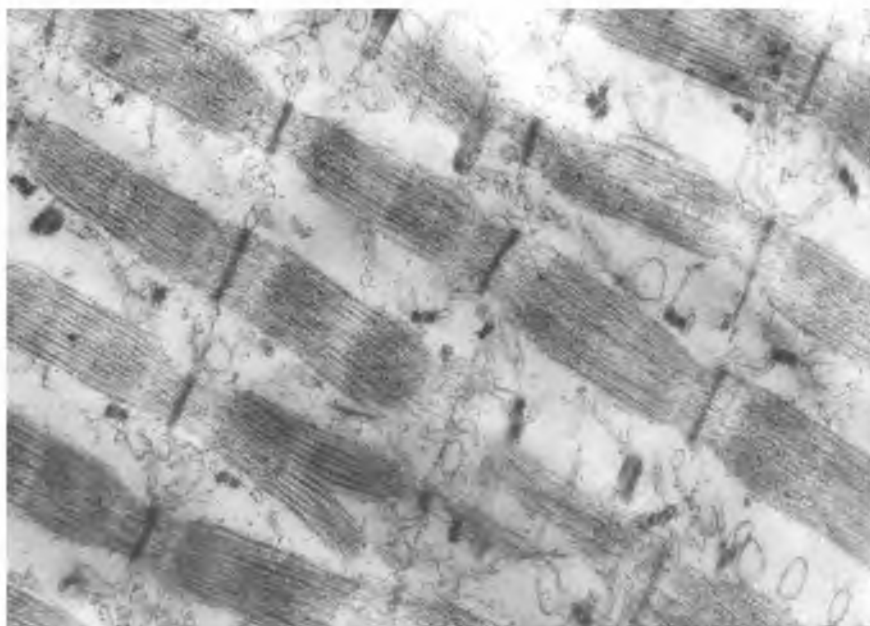


Fig. 2

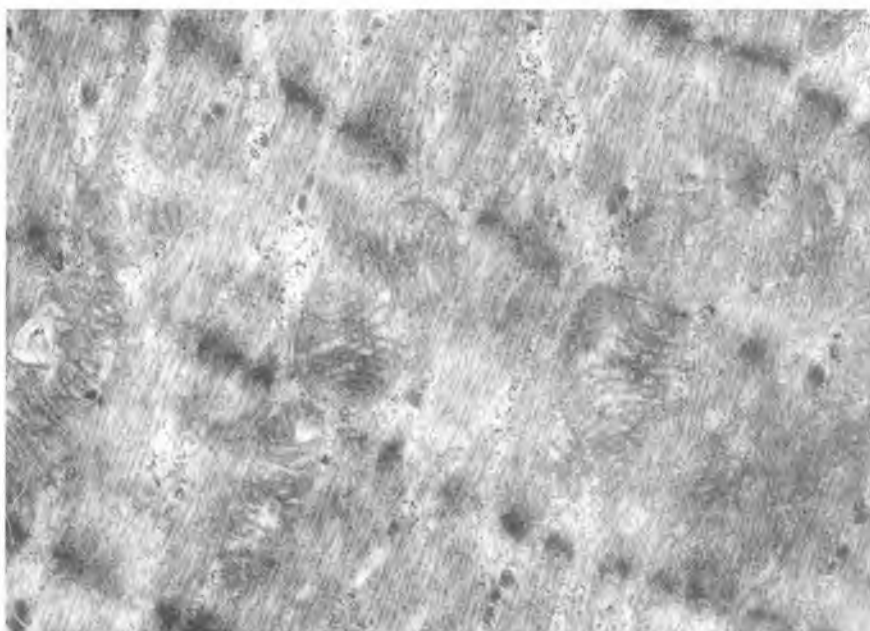


Fig. 3

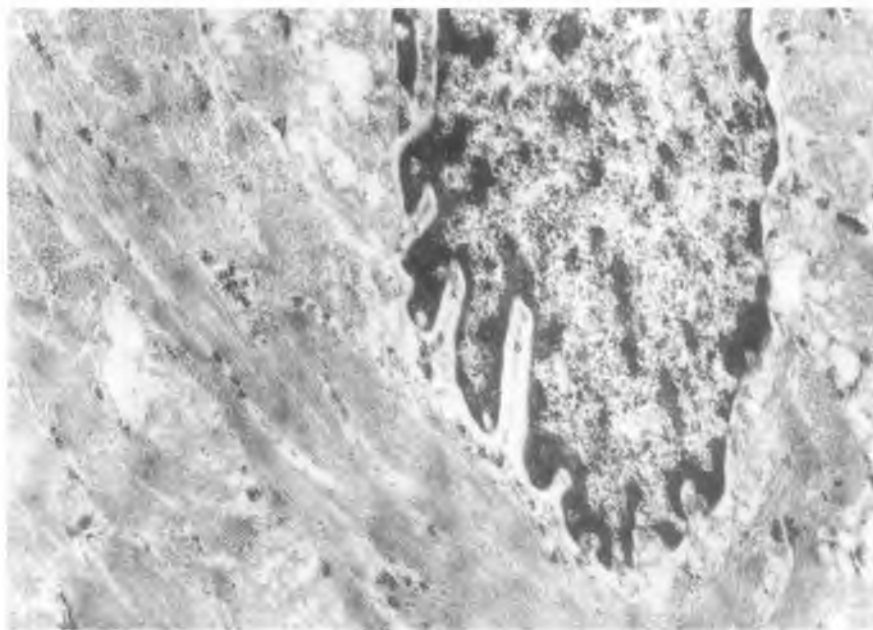


Fig. 4

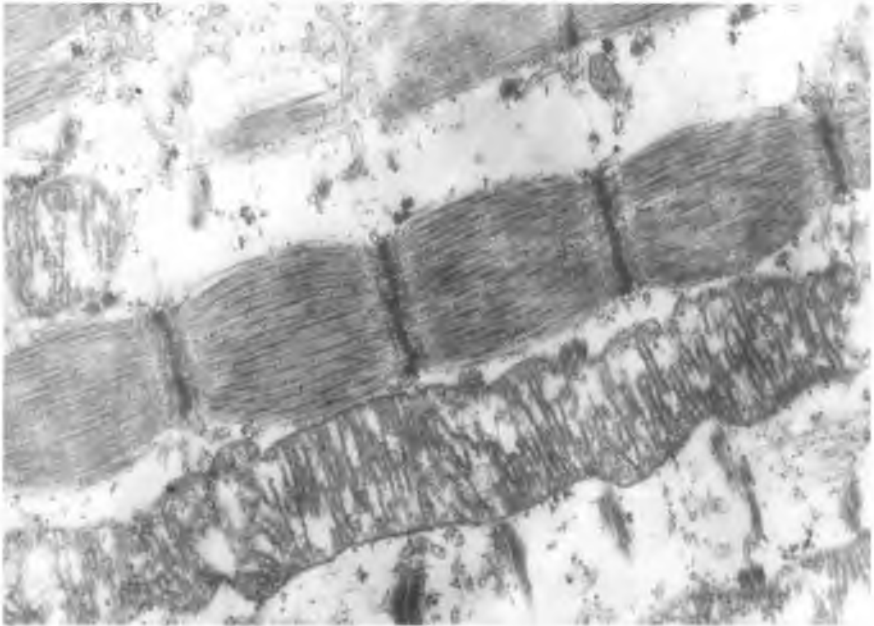


Fig. 5

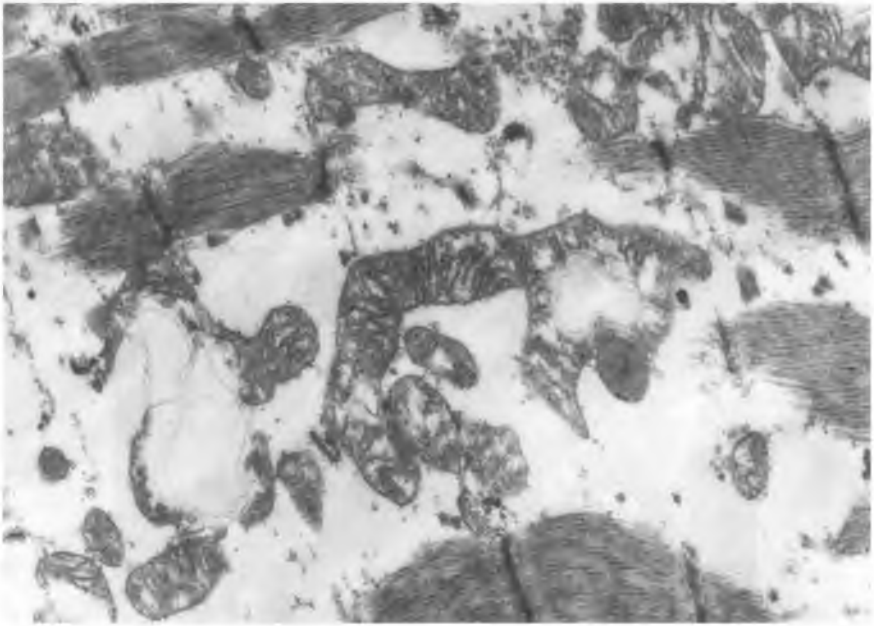


Fig. 6

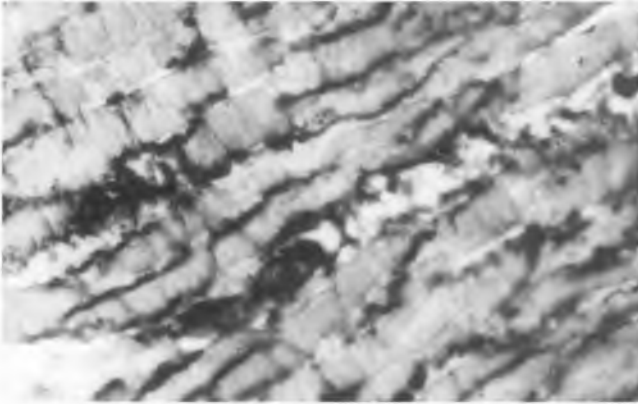


Fig. 7

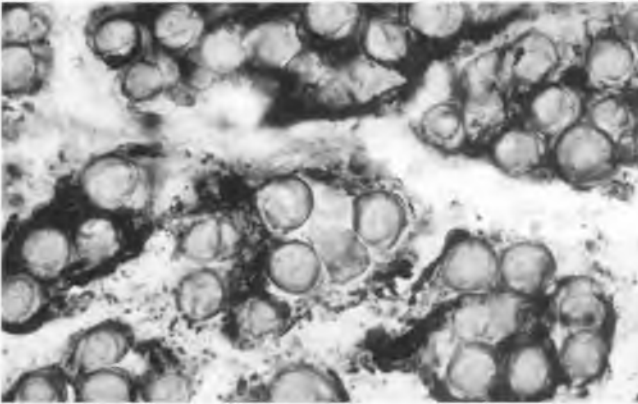


Fig. 8

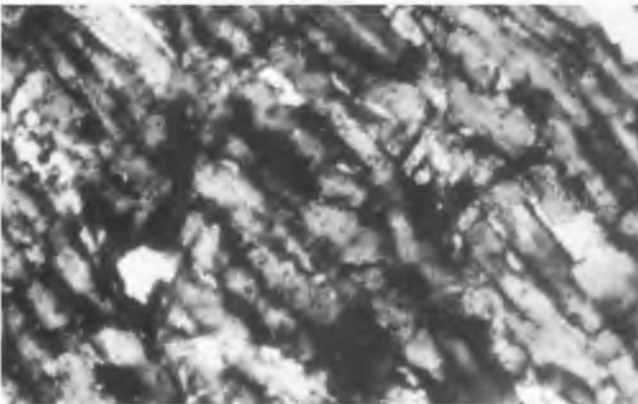


Fig. 9

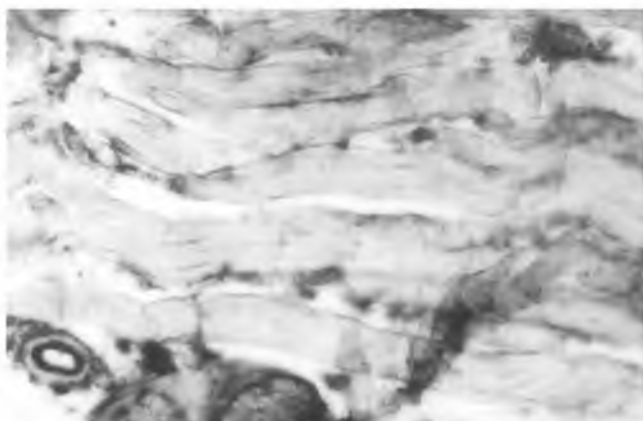


Fig. 10

